JOURNAL OF VIROLOGY, Nov. 1997, p. 8268–8278 Vol. 71, No. 11
0022-538X/97/$04.00+0

Rotavirus Is Released from the Apical Surface of Cultured Human Intestinal Cells through Nonconventional Vesicular Transport That Bypasses the Golgi Apparatus

NATHALIE JOURDAN,[1]* MICHÈLE MAURICE,[2] DANIÈLE DELAUTIER,[3] ANNE MARIE QUERO,[1] ALAIN L. SERVIN,[1] AND GERMAIN TRUGNAN[2]

Institut National de la Santé et de la Recherche Médicale, CJF 94 07, Pathogénie Cellulaire et Moléculaire des Microorganismes Entérovirulents, Faculté de Pharmacie, Université Paris XI, 92296 Chatenay-Malabry Cedex,[1] CJF 96 07, Signalisation Moléculaire et Physiopathologie de l'Adressage des Protéines dans les Cellules Épithéliales, Faculté de Médecine Saint Antoine, Université Paris VI, 75012 Paris,[2] and U 327, Structure et Fonction des Cellules Hépatiques, Faculté de Médecine X. Bichat, Université Paris 7, 75018 Paris,[3] France

Received 2 May 1997/Accepted 16 July 1997

Rotaviruses are nonenveloped viruses that infect enterocytes of the small intestine and cause severe infantile gastroenteritis. It was previously thought that rotavirus exits cells by lysis, but this behavior does not match the local pathogenesis of the virus. In this study, we have investigated the release of the simian rotavirus strain (RRV) from the polarized intestinal Caco-2 cells. We found that RRV is released almost exclusively from the apical pole of Caco-2 cells before any cells lyse. Using confocal laser scanning microscopy and drugs that inhibit vesicular transport, we studied the RRV transport route from the endoplasmic reticulum (ER) to the apical side of intestinal cells. We demonstrated that RRV exits from the ER through a carbonyl cyanide *m*-chlorophenylhydrazone-sensitive vesicular transport. RRV staining was never found within the Golgi apparatus or lysosomes, suggesting that the RRV intracellular pathway does not involve these organelles. This finding was confirmed by treatment with monensin or NH_4Cl, which do not affect release of RRV. Electron microscopic analysis revealed RRV containing small smooth vesicles in the apical area and free virions outside the cell in the brush border, consistent with a vesicular vectorial transport of virus. These results may provide, for the first time, a cellular explanation of the pathogenesis of rotavirus.

Rotaviruses are nonenveloped, double-stranded RNA viruses that are recognized as the leading cause of infantile viral gastroenteritis worldwide (22). Rotaviruses exhibit marked tropism for the differentiated enterocytes of the intestinal epithelium (5). The intestinal mucosa, like other epithelia, forms a highly organized sheet structure, separating the external lumen from the internal milieu, and it therefore represents the initial target for pathogens. Consequently, the vectorial release of virus is of essential importance for viral pathogenesis. Indeed, viruses released from the apical membrane of epithelial cells are likely to produce a localized infection restricted to the epithelial surface. In contrast, viruses released at the basolateral membrane can spread to underlying tissues and cause a more general infection (55, 56).

Most of our knowledge on virus release mechanisms derives from studies on enveloped viruses. Their vectorial release from polarized cells has been extensively investigated in vivo and with cultured epithelial cells. In 1978 Rodriguez-Boulan and Sabatini reported that enveloped RNA viruses are released from MDCK cells in a polar fashion; vesicular stomatitis virus budded predominantly from the basolateral plasma membrane, whereas Sendai virus and influenza virus virions were released exclusively from the apical domain (37). Type C retroviruses where also observed to be shed preferentially from the basolateral membrane of polarized epithelial cells (43), and more recently human immunodeficiency virus type 1 was found to be preferentially released from the basolateral surface of intestinal HT-29-D4 cells (14). More detailed analysis revealed that polarized viral budding is preceded by the polarized localization of viral envelope proteins in the plasma membrane (31, 36, 41, 43). Enveloped viruses that bud at intracellular membranes are also asymmetrically released from polarized epithelial cells. Herpes simplex virus, which matures from the inner nuclear membrane, was found to follow a vesicular transport process to the basolateral domain of several different type of polarized epithelial cells (46). Bunyavirus (2, 8) and coronavirus (39, 40) were also found to be released by a vectorial vesicular transport process.

In contrast, nonenveloped viruses have long been thought to be released following cell lysis (60); thus, their transport and release have been less thoroughly investigated. However, studies using simian virus 40 (SV40) (10) and poliovirus (61) have indicated that nonenveloped viruses may also be released before cell lysis, at a particular plasma membrane domain.

Rotavirus undergoes a unique maturation process. Immature subviral particles assemble in cytoplasmic viroplasm structures, bud through the endoplasmic reticulum (ER) membrane, and acquire a transient membrane envelope (32, 33). Subsequently, this membrane is lost (58), and the outer capsid protein VP7, retained in the ER, is folded into the subviral particles to form the definitive, mature viral particles (12). Until now, from studies using MA104 cells, rotaviruses were known to be retained in the ER lumen until cell lysis (1, 30). However, this nonpolarized embryonic rhesus monkey kidney cell line does not display any morphologic or functional characteristics of the rotavirus natural target cell. Moreover, viral spreading through cell lysis does not match recent data indicating that rotavirus may infect and multiply during more than

* Corresponding author. Mailing address: CJF INSERM 94 07, Faculté de Pharmacie, 5 rue J. B. Clément, 92296 Chatenay-Malabry Cedex, France. Phone and fax: 33-1 46 83 56 61.

one cycle of replication, without cell death or membrane leaks (52). This observation correlates with in vivo data demonstrating that rotavirus may replicate without any histopathologic changes (6, 57).

The human intestinal epithelial cell line Caco-2, established from a human colon adenocarcinoma (15), has been shown to spontaneously display, after confluency, many of the morphologic and biochemical properties of mature enterocytes (34). These characteristics include cellular polarization with two plasma membrane domains, an apical one which faces the external lumen and a basolateral one which faces the internal milieu. The apical domain is characterized by a brush border membrane and the expression of intestinal hydrolases (34). Caco-2 cells have been recognized as one of the most efficient enterocyte-like models for studying interactions between enteropathogens and the intestine (26, 27, 47). Moreover, our group and others have reported that a cell culture-adapted rhesus rotavirus (RRV) is able to infect differentiated Caco-2 cells (20, 23, 52).

In this study, we have investigated the transport and release of the simian rotavirus strain RRV from the polarized intestinal Caco-2 cells. We found that RRV was released almost exclusively at the apical pole of Caco-2 cells before any cell lysis was detected. Using confocal laser scanning microscopy, electron microscopy, and drugs that inhibit the vesicular transport, we studied the RRV transport pathway from the ER to the apical surface of intestinal cells. Our results describe for the first time the existence of a nonconventional vesicular transport of RRV particles, from the ER to the apical plasma membrane of Caco-2 cells, that bypasses the Golgi apparatus and lysosomes.

MATERIALS AND METHODS

Reagents. Carbonyl cyanide *m*-chlorophenylhydrazone (CCCP), monensin, 1,4-diazabicyclo-[2.2.2.]octane, trypsin, Triton X-100, and paraformaldehyde were purchased from Sigma (L'Isle d'Abeau Chesnes, France). Glycergel and propidium iodide were from DAKO (Dakopatts, Copenhagen, Denmark). Ammonium chloride was obtained from Prolabo (Paris, France). Products for cell culture were from Life Technologies (Eragny, France). Transwell filters (0.4-μm pore size) were obtained from Costar (Dominique Dutscher, Brumath, France). The bicinchoninic acid assay kit was purchased from Pierce (Interchim, Montluçon, France).

Cells and culture conditions. The Caco-2 cell line has been established from a human colon adenocarcinoma by J. Fogh (Memorial Sloan Kettering Cancer Center, Rye, N.Y.) (15). Cells were cultured (passages 60 to 90) in Dulbecco modified Eagle's medium supplemented with 20% heat-inactivated fetal bovine serum, 1% penicillin-streptomycin, and 1% nonessential amino acids (34). For viral infection studies, the cells were seeded at a density of 10,000 cells per cm^2 on tissue culture-treated polycarbonate Transwell filters containing pores of 0.4 μm in diameter. Apical and basal media were replaced at 2-day intervals from day 2. Infections were done late after confluency, i.e., after 20 days in culture. Maintenance of the cells was at 37°C in a 10% CO_2–90% air atmosphere.

MA104 cells were cultured as previously described (20).

Virus. RRV was obtained from J. Cohen (INRA, Jouy en Josas, France). Virus stock was generated in MA104 cells after a 24-h preincubation of the cells in a serum-free culture medium. Viruses were treated with 0.5 μg of trypsin per ml (9) at 37°C for 30 min, and MA104 cell monolayers were infected at a multiplicity of infection (MOI) of 0.002 PFU/cell. After 1 h of adsorption at room temperature, the inoculum was removed and infected cells were incubated in a culture medium containing 0.5 μg of trypsin per ml. After complete cytopathic effect was obtained, the cultures were freeze-thawed and cell debris were removed by centrifugation.

Virus infection on filters. A virus inoculum was activated for 30 min by treatment with 0.5 μg of trypsin per ml (9), and Caco-2 cells grown on Transwell filters (cultured without fetal bovine serum for 24 h) were apically infected with an inoculum at an MOI of 10 PFU/cell in apical chambers for 1 h at room temperature. The inoculum was then removed, and fresh medium containing 0.5 μg of trypsin per ml was added. Infected cells were incubated at 37°C in a 10% CO_2–air atmosphere and were processed for experiments at 16, 18, 20, or 24 h postinfection (p.i.). In some experiments cells were infected through the basolateral chambers. No difference in RRV replication and release under the two conditions of infection was observed.

Measurement of virus release. Apical or basolateral cell culture media from infected filter-grown Caco-2 cells were collected, and the titers of released virus were determined by plaque assay on MA104 cells as previously described (13). The cell-associated virus was removed from cells by two cycles of freeze-thawing. The cell debris was pelleted by centrifugation at 600 × *g*, and virus titers present in the supernatant were determined by plaque assay.

Measurement of cell viability and monolayer integrity. (i) Desquamation. The desquamated cells from infected and mock-infected Caco-2 monolayers were counted with a hemocytometer.

(ii) Measurements of transepithelial electrical resistance. Transepithelial electrical resistance of polarized infected and mock-infected Caco-2 cells grown on Transwell filters was measured by using a Millicell-ERS apparatus (Millipore S. A., Saint-Quentin en Yvelines, France). Results were expressed as ohms times square centimeters.

(iii) LDH release. The lactate dehydrogenase (LDH) activity in the culture medium was assayed by measuring the oxidation of NADH with pyruvate as a substrate at 340 nm with an Enzyline LDH kit (Biomerieux, Paris, France) according to the manufacturer's instructions. Protein was assayed with the bicinchoninic acid assay (Pierce). Results were expressed as milliunits of LDH activity per milligram of protein in cell monolayers.

Antibodies and lectin. Rabbit polyclonal antirotavirus antibody (8148) was a gift from Jean Cohen. Rat monoclonal anti-dipeptidyl peptidase IV (anti-DPP IV) antibody (4H3) was a gift from Suzanne Maroux (17). Mouse monoclonal anti-Lamp-1 antibody (BB6) was a gift from S. R. Carlsson (7). Mouse monoclonal anti-protein disulfide isomerase (anti-PDI) antibody was obtained from StressGen (Tebu, Le Perray en Yvelines, France). Fluorescein isothiocyanate (FITC)-conjugated rabbit anti-rat immunoglobulin G (IgG) was purchased from Sigma. Tetramethyl rhodamine isothiocyanate (TRITC)-conjugated goat anti-rabbit IgG was from Biosys (Compiègne, France). FITC-conjugated goat anti-mouse IgG was purchased from Jackson ImmunoResearch Laboratories (Interchim). FITC-conjugated wheat germ agglutinin was obtained from Biovalley (Conches, France).

Immunofluorescence and confocal laser scanning microscopy. Caco-2 cells cultured on Transwell filters were fixed with 2% paraformaldhehyde for 15 min at room temperature, washed three times with phosphate-buffered saline (PBS), and then permeabilized with 0.2% Triton X-100 in H_2O. After three washes in PBS, they were stained for RRV, DPP IV, PDI, or Lamp-1 by incubation with the antibodies described above for 60 min at room temperature. After three washes in PBS, incubation with an FITC- or TRITC-conjugated second antibody was performed for 45 min. For double labeling, the respective antibodies were applied sequentially. After the last wash, fixed cells were incubated for 10 min with 1,4-diazabicyclo-[2.2.2.]octane antifading reagent and mounted with glycergel. Fluorescence was observed with a Leica TCS equipped with a DMR inverted microscope and a 63/1.4 objective. A krypton-argon mixed-gas laser was used to generate two bands: 488 nm for FITC and 568 nm for TRITC. A band pass filter was used to recover FITC fluorescence, and an LP 590 filter was used for TRITC. Both fluorochromes were excited and analyzed in one pass with no interference between the two channels. Image processing was performed with the on-line Scan Ware software. Numeric images were transferred on a Power Mac 8100 equipped with an image analysis station (Image 1.57 and Photoshop), and mounted images were printed on a Kodak XLS 8600 PS printer.

Electron microscopy. Filters were rinsed three times with PBS, and the cells were fixed with 2.5% glutaraldehyde in 0.1 M sodium phosphate buffer (pH 7.4) for 30 min at room temperature. After being washed with PBS, they were postfixed for 30 min at room temperature with 1.5% osmium tetroxide in sodium phosphate buffer. The filters were then dehydrated in a graded ethanol series, cut into strips, and embedded in epoxy resin. Ultrathin sections were double stained with uranyl acetate and lead citrate and examined with a Jeol JEM-1010 electron microscope.

RESULTS

RRV is released almost exclusively from the apical domain of intestinal polarized Caco-2 cells before cell lysis. In order to determine whether RRV release from Caco-2 cells is polarized and to establish the time course of virus release, the apical and basolateral media of RRV-infected Caco-2 cells were examined for yields of progeny virus. At various times after infection of filter-grown Caco-2 cells, the virus titers in the apical and basolateral culture media were determined. Intracellular progeny virus not yet released was also quantitated. As seen in Table 1, an almost exclusive apical release of RRV from the Caco-2 cells was observed at 18, 20, and 24 h p.i., with virus titers in the apical chambers representing 99.9% of the extracellular virus. The time course study reveals that the release increased from 18 to 24 h p.i., a time at which less than 4% of virions were detectable in cell monolayers. At 48 h p.i., basolateral virions represented 16% of total released virions, and by

TABLE 1. Release of RRV from polarized Caco-2 cells and nonpolarized MA104 cells[a]

Virus location	Virus titer (PFU/ml)[b]					
	Caco-2 cells					MA104 cells (24 h)
	18 h	20 h	24 h	48 h	72 h	
Apical	$(5.6 \pm 0.25) \times 10^7$	$(6.4 \pm 0.18) \times 10^7$	$(7.15 \pm 0.6) \times 10^7$	$(6.01 \pm 0.55) \times 10^7$	$(3.62 \pm 0.3) \times 10^7$	$(5.5 \pm 0.18) \times 10^7$
Basolateral	$(6.2 \pm 1.0) \times 10^3$	$(9 \pm 1.0) \times 10^3$	$(2 \pm 0.29) \times 10^4$	$(1.15 \pm 0.19) \times 10^7$	$(3.71 \pm 0.22) \times 10^7$	$(5.8 \pm 0.15) \times 10^7$
Intracellular	$(1.4 \pm 3.5) \times 10^7$	$(0.7 \pm 0.14) \times 10^7$	$(0.15 \pm 0.03) \times 10^7$	$(7.5 \pm 1.2) \times 10^5$	$(9 \pm 1.0) \times 10^4$	$(10 \pm 1.0) \times 10^4$
Total[c]	$(7 \pm 0.58) \times 10^7$	$(7.1 \pm 0.28) \times 10^7$	$(7.3 \pm 0.64) \times 10^7$	$(7.2 \pm 0.69) \times 10^7$	$(7.34 \pm 0.51) \times 10^7$	$(1.1 \pm 0.2) \times 10^8$

[a] Monolayers of 20-day-old Caco-2 cells or 6-day-old MA104 cells grown on Transwell filters were infected with RRV at an MOI of 10 PFU per cell. At 18, 20, 24, 48, and 72 h p.i., media were collected from the apical and basolateral chambers and assayed for virus titration by plaque assay. Intracellular virus was removed from cells by two cycles of freeze-thawing. The cell debris were pelleted by centrifugation, and virus titers present in the supernatant were determined by plaque assay.

[b] Values are means ± standard deviations from at least 10 experiments.

[c] Total virus titers represent the sum of the extracellular and intracellular virus titers for each time. The total virus titer at 2 h p.i. was determined and was found to be less than 10 PFU/ml.

72 h p.i., the same quantities of virions were detected in the apical and basolateral chambers. It should be noted that at 48 and 72 h p.i., the total yield of progeny virus was not significantly higher than that released at 24 h p.i. As early as 24 h p.i., RRV was released at similar levels in both the apical and basolateral media of nonintestinal and nonpolarized filter-grown MA104 cells.

To gain more information about RRV release, we observed Caco-2-infected cells by using confocal laser scanning microscopy. Caco-2 cells were fixed with paraformaldehyde, permeabilized with Triton, and double labeled with a polyclonal anti-group A rotavirus antibody and a monoclonal antibody directed against DPP IV, a brush border intestinal hydrolase specifically located at the apical plasma membrane (59). The distributions of RRV and DPP IV were analyzed at 24 h p.i., and both were found at the apical surface (Fig. 1A). Figure 1B shows the release of virions from an intact apical brush border. These observations correlated well with the quantitative data described above.

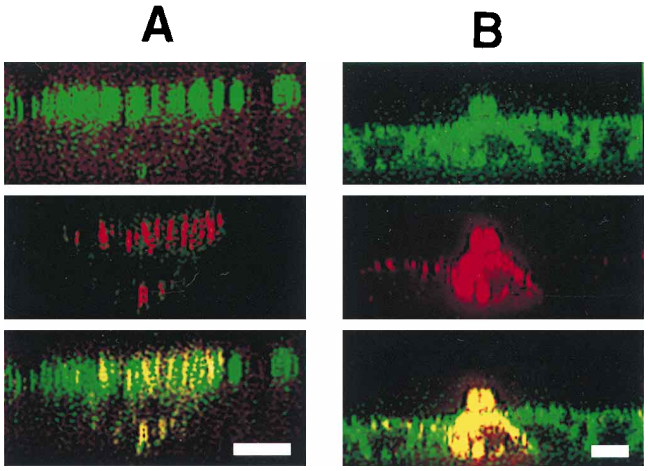

FIG. 1. Apical localization of RRV virions at 24 h p.i. by indirect double immunofluorescence labeling. Infected cells were fixed in 3% paraformaldehyde and permeabilized with 0.1% Triton X-100. RRV virions were immunostained with polyclonal anti-group A rotavirus antibodies and rhodamine-labeled anti-rabbit IgG antibodies (middle). The apical marker DPP IV brush border hydrolase was stained with rat monoclonal anti-DPP IV and fluorescein-coupled anti-rat IgG antibodies (top). Colocalization of the two fluorophores (bottom) was revealed by the yellow color. Vertical sections (*xz*) of infected Caco-2 cells were obtained by direct confocal analysis. (A) RRV labeling is associated predominantly with the apical surface of the cells. (B) It was possible to observe RRV virions being released from an intact apical brush border in some randomly distributed cells of the monolayer. Bars, 20 μm.

We investigated cell viability and monolayer integrity at 24, 48, and 72 h p.i. As assessed by transepithelial resistance (Fig. 2A) or by cell desquamation (Fig. 2B), there was no significant change in monolayer integrity within the first 24 h p.i. Moreover, the very low LDH release measured in the apical medium revealed no loss of membrane integrity at 24 h p.i. (Fig. 2C). Monolayer disruption and membrane injury were detectable only from 48 h p.i.

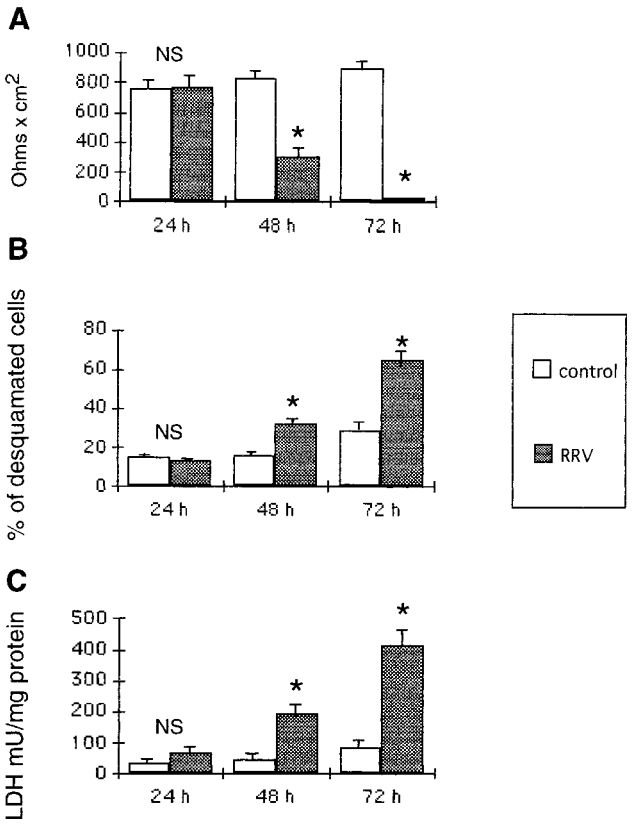

FIG. 2. Time course of cell viability and monolayer integrity. Monolayers of 20-day-old Caco-2 cells grown on Transwell filters were infected with RRV at an MOI of 10 PFU per cell. Infected and mock-infected cells were assayed at indicated times p.i. for transepithelial electrical resistance (A), numeration of desquamated cells (B), or LDH release (C). Values are means ± standard deviations from at least 10 experiments. Statistical differences between control and infected cells were determined by Student's *t* test. NS, not significantly different. *, $P < 0.05$.

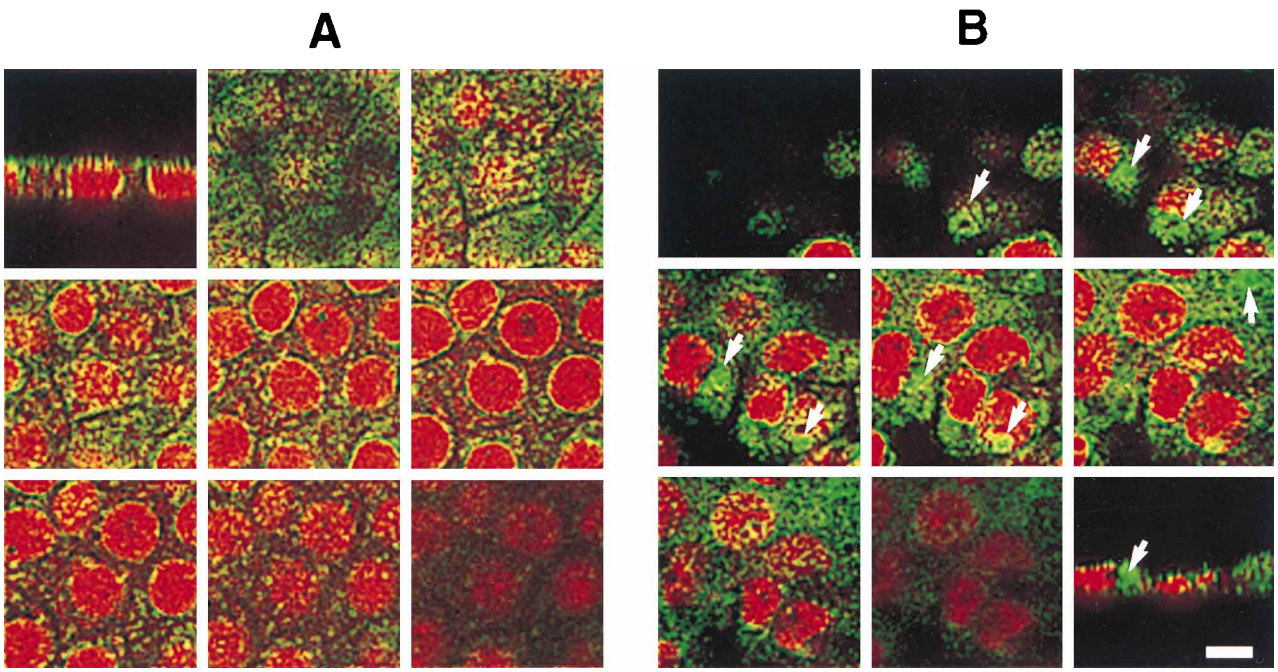

FIG. 3. Immunofluorescence analysis of the ER in noninfected (A) and infected (B) Caco-2 cells. Cells were fixed and permeabilized as described in the legend to Fig. 1. The ER marker PDI was stained with mouse monoclonal anti-PDI and fluorescein-coupled anti-mouse IgG antibodies. The nucleus was stained red with propidium iodide. Vertical sections (*xz*) (top left in panel A and bottom right in panel B) and successive horizontal sections (*xy*) of 2 μm from the apical to the basal surfaces of the cells (top to bottom) were obtained by confocal laser scanning analysis. (A) Regular ER structures at the top of the nucleus. (B) At 16 h p.i., RRV induces a dramatic change in the ER. Arrows, dilated ER structures. Bars, 15 μm.

Together these data indicate that rotavirus is released efficiently from the apical surface of Caco-2 cells at 24 h p.i., before cell lysis and monolayer disruption, which take place at 48 and 72 h p.i.

RRV particles exit from the ER through a CCCP-sensitive event. The intracellular pathway of RRV between the ER and the apical plasma membrane was investigated by using immunofluorescence staining. In mock-infected Caco-2 cells, PDI, a luminal ER resident protein, was found as expected in vesicular structures organized in a polarized fashion mostly at the top of the nucleus (Fig. 3A). Rotavirus infection induced dramatic changes in the ER structure as early as 16 h p.i. The PDI antibody stained irregular vesicular structures that corresponded to an obvious ER swelling (Fig. 3B). However, the perinuclear distribution of the ER is conserved, as can be seen on the vertical section (Fig. 3B). By using double labeling, it was possible to show that ER swelling was caused by RRV accumulation (Fig. 4A), whereas the ER displayed a normal structure in noninfected neighboring cells. Interestingly, at 18 h p.i. (not shown) and more obviously after 24 h p.i., RRV and ER staining were clearly distinct (Fig. 4B), thus suggesting that viral particles had been transported out of the ER. This was confirmed by using CCCP, an uncoupler of oxidative phosphorylation, which is known to block transport out of the ER because this is an ATP-dependent event (54). RRV-infected Caco-2 cells were incubated from 16 to 24 h p.i. with 10 mM CCCP, which was added late enough during the replication cycle of RRV in Caco-2 cells so as not to affect viral replication, protein assembly, or maturation by budding through the ER membrane. At 24 h p.i., in untreated RRV-infected cells, PDI and rotavirus particles were no longer found in the same structures (Fig. 4B). By contrast, PDI and rotavirus particles were still completely colocalized in CCCP-treated cells (Fig. 4C). Cells were also assayed at 20 and 24 h p.i. for titration of apical, basolateral, and intracellular progeny virus. Between 20 and 24 h p.i., while in control cells intracellular virions decreased and apical virions increased, in CCCP-treated cells apical release was completely blocked and virions were maintained intracellularly (Fig. 5A). These results indicate that CCCP treatment efficiently inhibited extracellular release of newly synthesized RRV particles. It should be noted that the total amount infectious virus recovered in the cell supernatants and within cells was not significantly different in CCCP-treated cells compared to untreated ones (Fig. 5B), indicating, as expected, that CCCP treatment did not affect virion replication, assembly, and maturation.

RRV particles bypass the Golgi apparatus. In order to identify a possible acceptor compartment for RRV particles between the ER and the apical membrane, we performed double labeling of RRV particles and the Golgi apparatus. The Golgi apparatus was labeled with the wheat germ agglutinin lectin, which interacts with oligosaccharides decorating glycoproteins trimmed in the Golgi stacks (53). No colocalization between RRV and the Golgi apparatus could be observed (not shown), therefore suggesting that transport of RRV to the apical surface does not pass through the Golgi apparatus. This was confirmed by using monensin, a sodium ionophore known to inhibit vesicular budding from the Golgi complex (35). RRV-infected Caco-2 cells were incubated from 16 to 24 h p.i. with 10 mM monensin and were assayed for intracellular and extracellular virus. Monensin treatment did not block virus release, since at 20 h p.i., only 10% of the total progeny virus remained intracellular and the virus was almost completely released between 20 and 24 h in treated as well as untreated cells (Fig. 5A). It was particularly interesting that the monensin treatment impaired the vectorial release of RRV. Indeed, at 20 h p.i. 14.7% of the total virus was detected in the basolateral medium, while only 0.01% was detected in control cells. Fur-

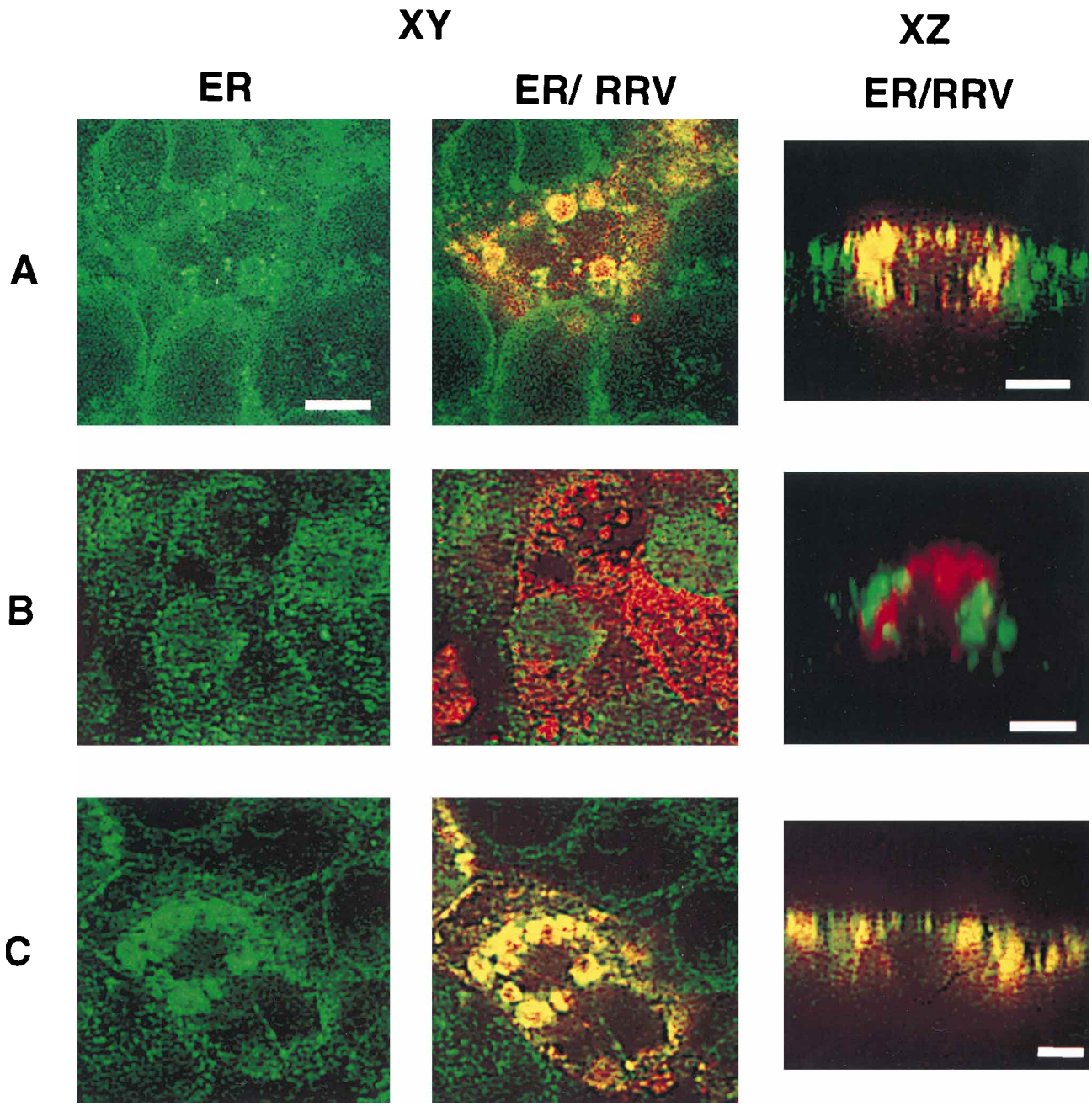

FIG. 4. RRV and ER localization at 16 h p.i. (A) and 24 h p.i. (B) in infected cells or at 24 h p.i. in infected cells treated with CCCP (C). At the indicated times p.i., cells were fixed, permeabilized, double stained by indirect immunofluorescence, and analyzed by confocal microscopy. RRV virions were immunostained with polyclonal anti-group A rotavirus antibodies and rhodamine-labeled anti-rabbit IgG antibodies. The ER marker PDI was stained with mouse monoclonal anti-PDI and fluorescein-coupled anti-mouse IgG antibodies. For each line the same horizontal focus (*xy*) is shown, displaying ER distribution (left) or ER and RRV distributions (middle). ER and RRV distributions on a vertical section (*xz*) are shown on the right. (A) In a focus plane obtained at the nucleus level, ER labeling reveals dilated ER structures. At 16 h p.i., RRV labeling is exactly localized in these dilated structures. Colocalization is demonstrated by the yellow color in horizontal and vertical sections. (B) At 24 h p.i., RRV staining is localized mainly in a focus plane obtained above the nucleus. Horizontal and vertical sections reveal the segregation of ER and RRV labels. Moreover, the vertical section shows RRV label greater than that of the ER, suggesting that RRV exits from the ER. (C) Upon CCCP treatment, even after 24 h p.i., RRV labeling still colocalizes within the dilated ER structure, suggesting that CCCP inhibits RRV exit from the ER. Bars, 10 μm.

thermore, between 20 and 24 h p.i. equal quantities of virus had been released in the apical and the basolateral media (Fig. 5A). Like for CCCP, monensin treatment did not affect virion replication, assembly, and maturation, since the same amounts of total infectious virus were recovered in monensin-treated and untreated cells (Fig. 5B).

RRV particles do not transit through the lysosomal compartment. Whether the intracellular route of RRV virions includes a transient passage within lysosomes was determined by immunolabeling of Lamp-1, a well-known lysosomal membrane protein (7). In mock-infected Caco-2 cells, Lamp-1 staining revealed numerous small vesicles spread throughout

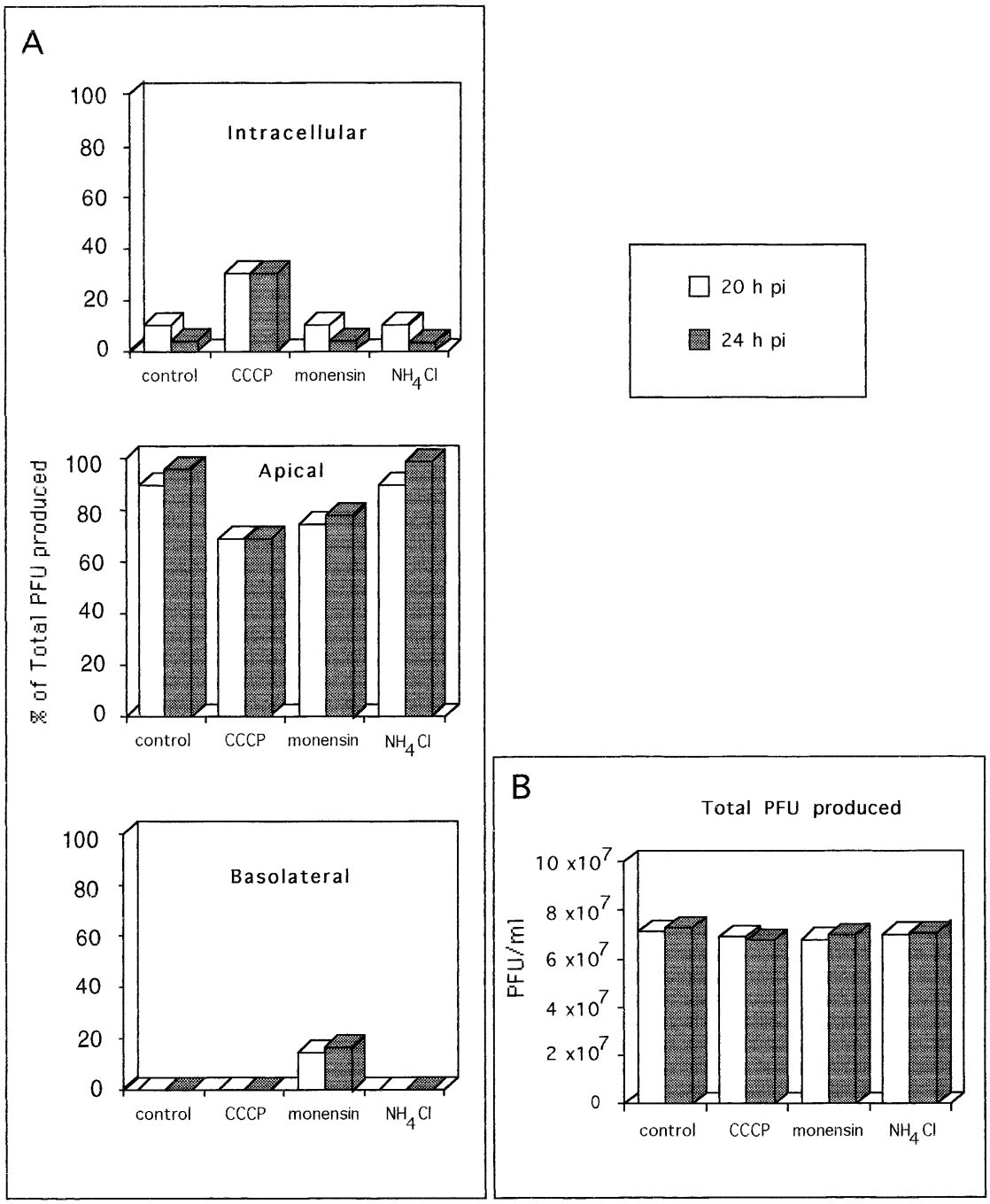

FIG. 5. Effect of CCCP, monensin, and NH_4Cl on RRV release. At 16 h p.i., cells were untreated (control) or treated with 10 mM CCCP, 10 mM monensin, or 50 mM NH_4Cl. (A) At 20 and 24 h p.i., the titers of apical released virus, basolateral released virus, and intracellular virus were determined by plaque assay. Results are expressed as the percentages of total infectious virus (B) recovered in cells and supernatants for each treatment. Each value is an average from five experiments.

the cytoplasm (Fig. 6A), as previously shown (4). Although the size of the lysosomes was more heterogeneous in RRV-infected cells (Fig. 6B) than in control cells, it was not possible to show any colocalization between RRV and Lamp-1 (Fig. 6C). This was confirmed by using NH_4Cl, a lysomotropic weak base known to have an inhibitory effect on lysosome functions (19). When RRV-infected Caco-2 cells were incubated from 16 to 24 h p.i. with 50 mM NH_4Cl, double immunostaining did not reveal any colocalization of rotavirus and lysosome markers (Fig. 6D and E). Moreover, virus titers in the apical and basolateral chambers were not changed by NH_4Cl treatment (Fig. 5A). All these observations argue against the transport of RRV virions through lysosomes.

Intracytoplasmic virions are restricted to vesicular structures; extracellular virions are free. To gain further insight into the intracellular pathway of RRV particles from the ER to the apical plasma membrane, infected Caco-2 cell monolayers were examined by electron microscopy between 20 and 24 h p.i.

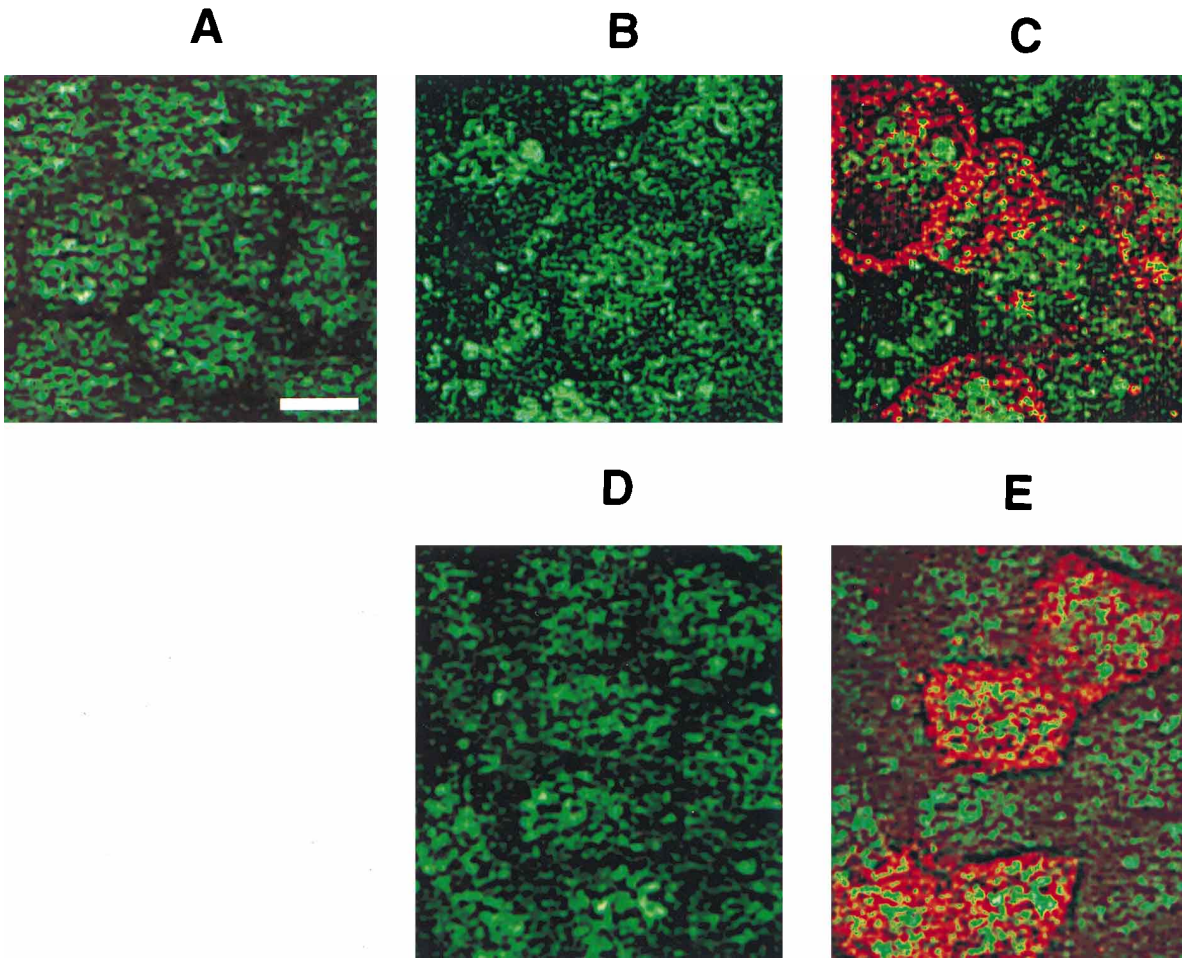

FIG. 6. RRV and lysosome localization. At 24 h p.i., cells were fixed, permeabilized, and analyzed by double-staining indirect immunofluorescence confocal microscopy. RRV virions were immunostained with polyclonal anti-group A rotavirus antibodies and rhodamine-labeled anti-rabbit IgG antibodies. The lysosome marker Lamp-1 was stained with mouse monoclonal antibody and fluorescein-coupled anti-mouse IgG antibodies. (A) In noninfected cells, lysosome staining reveals numerous small vesicles spread throughout the cytoplasm. (B) In infected cells, the sizes of lysosomes appear to be heterogeneous. (C) The superposition of RRV and lysosome staining shows the total exclusion of the two labels. (D and E) In RRV-infected cells treated with NH_4Cl, RRV, and Lamp-1, the labels still exclude each other. Bar, 10 μm.

Tight junctions and the plasma membrane appeared to be intact, and the microvilli lining the apical surface appeared roughly normal, with, however, some irregular or distorted shape. Electron-dense viral particles were seen in ER structures around the nucleus (Fig. 7A). Higher magnification of the perinuclear region (Fig. 7B) showed the accumulation of virion particles within dilated cisternae of the rough ER, in accordance with previous studies showing that rotavirus particles mature and accumulate in dilated ER cisternae (1). Clustered small, smooth vesicles enclosing one to three mature virion particles were observed in the apical area (Fig. 7C). These virion-containing vesicles were also observed under the terminal web (Fig. 7D). In agreement with immunostaining data, virion particles were never observed within the Golgi apparatus (Fig. 7A). Extracellular progeny viruses, which had probably been recently released from the cells, were free (Fig. 7D) and scattered between microvilli of the brush border. Together, these ultrastructural observations suggest that new RRV virions are transported from the ER to the apical plasma membrane by a vesicular transport process.

DISCUSSION

The availability of epithelial cells in culture has provided a powerful tool for investigators interested in interactions of viruses with epithelial surfaces (for a review, see reference 60). In this study, the transport and release of rotavirus were investigated by using the epithelial intestinal cell line Caco-2, which closely mimics enterocytes, thus allowing in vitro studies on the interaction of rotavirus with a cellular model that resembles their in vivo natural target. The results demonstrate that newly synthesized RRV particles are released almost exclusively from the apical domain of Caco-2 cells, before any cell lysis or disruption of monolayers. In addition, RRV particles are transported from the ER to the apical plasma membrane by an atypical vesicular transport process that bypasses the Golgi apparatus and lysosomes.

Nonenveloped viruses, such as rotaviruses, have been generally considered to be released by lysis of the infected cells (60). Our data clearly demonstrate that transmembrane leakage and cell viability are altered only after 24 h p.i., when total progeny viruses have already been released. Release without

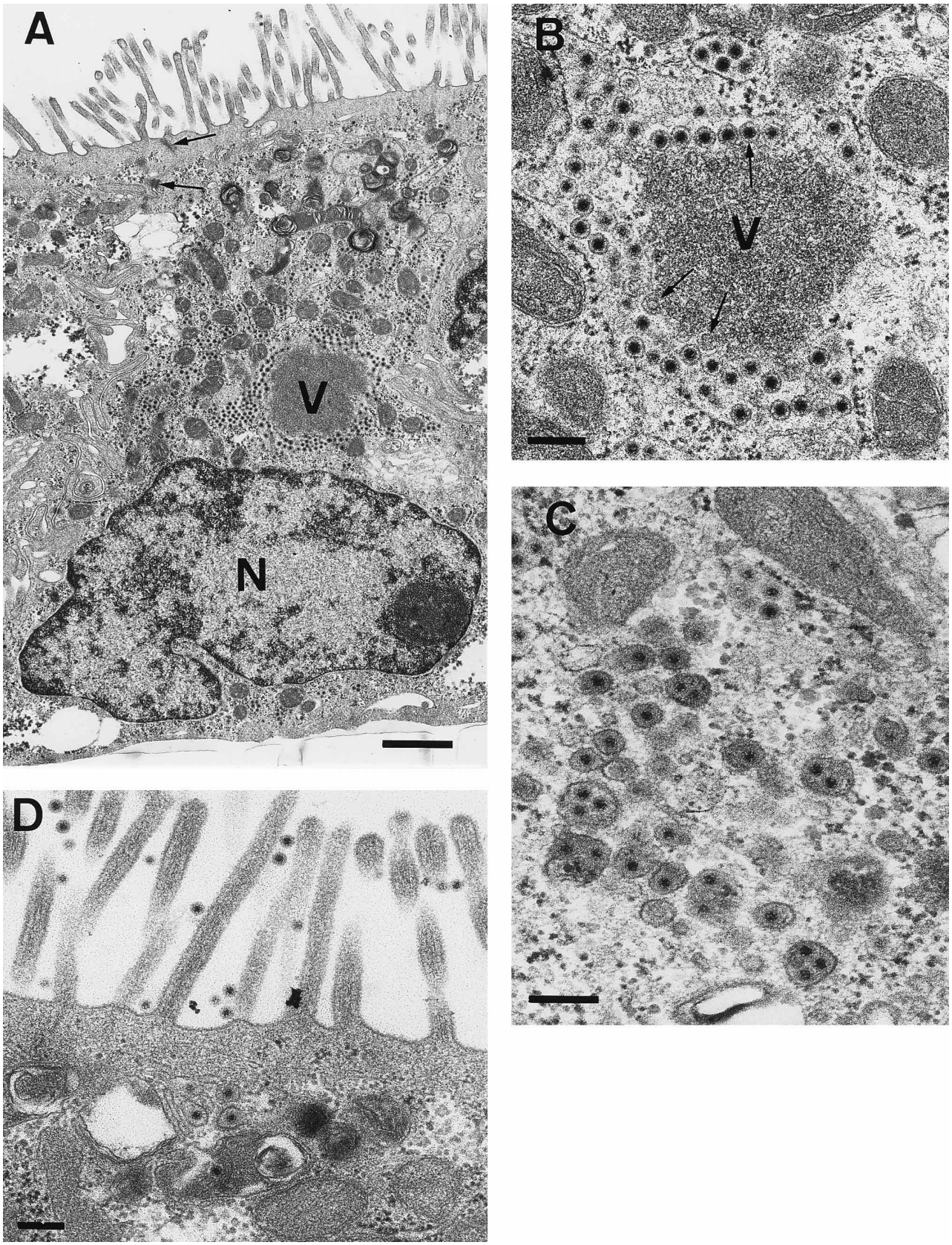

FIG. 7. Electron microscopy analysis of infected Caco-2 cells. At 24 h p.i., cells were fixed and embedded as described in Materials and Methods. Thin sections were cut orthogonally to the filter, and after staining to improve contrast, samples were visualized by electron microscopy. (A) Infected Caco-2 cell exhibiting a typical enterocyte-like appearance with an apical brush border, microvilli, and typical tight junctions and desmosomes (arrows). N, nucleus; V, viroplasm. (B) Higher magnification of a perinuclear region showing RRV particles accumulated within dilated rough ER cisternae. Arrows point to virus particles budding from viroplasm into the rough ER. (C) Part of the apical region of the cell showing RRV virions enclosed within smooth membrane vesicles. (D) Similar vesicles containing virus just under the terminal web. Extracellular virus is free and scattered between microvilli. Bars, 1 μm (A) and 200 nm (B, C, and D).

cell lysis or transmembrane leaks is consistent with some in vivo observations indicating that rotavirus may replicate without any histopathologic changes (6, 57). However, Svensson et al. observed an abolition of the electrical resistance of RRV-infected Caco-2 monolayers at 18 to 24 h p.i. and concluded that a transmembrane leak occured before the onset of viral release (52). This discrepancy may be due to the fact that we used Caco-2 cells grown for 20 days instead of 14 days. Under these conditions, cells display higher electrical resistance, suggesting that intercellular junctions are fully closed (3). Two other nonenveloped viruses, SV40 and poliovirus, have also been observed to be released from the apical surfaces of epithelial cells before the destruction of individual cells within intact monolayers. This common feature suggests that nonenveloped viruses require an intact host cell surface or intact host cell machinery to be released.

Since new RRV virions are released without cell lysis, how do they exit the cell? Present data show that after accumulation in the ER, RRV particles exit from this organelle by a CCCP-sensitive vesicular transport pathway, which is different from the secretory pathway, since it does not involve the Golgi complex. This finding is in accordance with previous electron microscopic studies that never found any rotavirus particles in Golgi stacks (1). Furthermore, the oligosaccharides present in the rotavirus external capside protein VP7 contain only high-mannose carbohydrates and remain endo-β-*N*-acetylglucosaminidase H sensitive, consistent with a Golgi bypass (21). Moreover, it has recently been reported that brefeldin A treatment of rotavirus-infected cells induces VP7 processing by Golgi enzymes but leads to the production of noninfectious rotavirus particles, suggesting that the VP7 protein of infectious rotavirus particles is not processed by Golgi enzymes and thus never transits through the Golgi apparatus (28). The hypothesis of a transient passage of an RRV particle, along its transport route, within lysosomes was refuted by the distinct localization of RRV staining and Lamp-1 staining in NH_4Cl-treated or untreated Caco-2 cells. Although rotavirus particles have been observed in lysosome-like structures by others (1), this probably does not represent a normal exit pathway of virions but rather represents an autophagic process where cells react against infection by lysosomal degradation.

Since RRV virions did not follow a classical exocytic pathway, what could be the vesicles that ensure their transport between the ER and the apical surface? The smooth membrane vesicles observed by electron microscopy represent potential candidates. They contained only mature virions and were observed in the apical area of cells. Our observations strongly suggest that these RRV transport vesicles probably fuse with apical plasma membrane and would release free virions in the extracellular medium. However, we have never observed a vesicle fusing with the plasma membrane. These RRV-containing vesicles have always been observed in cells that also contained viroplasms. Thus, they are unlikely to correspond to virions internalized at the apical surface, since it has been well established that cells actively producing virus cannot be reinfected. Moreover, they differed from the endocytic vesicles observed by Suzuki et al. (51), by both their morphological characteristics and their distributions (clustered vesicles versus isolated vesicles). Such a vesicular transport from the ER to the cell surface that bypasses the Golgi apparatus has rarely been described before. To our knowledge, only SV40 seems to also follow an atypical vesicular transport process, since virions have been observed in cytoplasmic smooth membrane vesicles just before apical release without any passage within the Golgi complex (10). Very recently, two proteins of enveloped viruses have also been observed to follow an atypical transport process. The Moloney murine leukemia virus Gag precursor (48) and the herpes simplex virus type 1 structural protein VP22 (11) are targeted to the cell surface via a nonclassical Golgi-independent mechanism. These observations and ours emphasize the interest in using viruses to explore new intracellular trafficking pathways.

RRV-containing vesicles presumably require targeting information to travel to the apical surface. Two kinds of mechanisms may be involved, which concern the sequence of viral proteins and/or the interaction of virions, or virion-containing vesicles, with the cellular targeting machinery. The presence of an apical targeting sequence has been extensively studied in the case of viral envelope proteins. An apical sorting signal in the ectodomain of the influenza virus hemagglutinin has been demonstrated (25, 41, 42), and more recently, Kundu et al. have identified a transmembrane domain sequence responsible for the apical transport of the influenza virus neuraminidase (24). Whether rotaviruses, although nonenveloped, use this strategy may be investigated by studying the transport pathway of rotavirus proteins expressed in Caco-2 cells by transfection, as has already been done for several enveloped-virus proteins in MDCK cells (18, 41, 42). The other, nonexclusive, possibility is that RRV utilizes an endogenous cellular targeting machinery. It is now established that apical targeting in Caco-2 cells is at least partially dependent on detergent-insoluble microdomains, which are highly enriched in glycosphingolipids (GSL) (16, 29). Interestingly, there is considerable evidence showing that to enter the cells, rotavirus does not utilize a cellular protein receptor but binds to GSL structures such as asialo-GM1 or GA1 (62) or to gangliosides present at the cell surface (38, 50). More recently, a study using the human enterocyte-like HT-29 cell line indicated that glycolipids containing specific carbohydrate moieties, such as sialic acid and galactose, contribute to the SA-11 rotavirus receptor structure (49). Preliminary studies from our laboratory have shown that after Caco-2 cell infection, RRV proteins are detected in the Triton X-100-insoluble fraction (unpublished data), suggesting that rotavirus-containing vesicles interact with GSL microdomains. Experiments using monensin provide strong support for this hypothesis. Indeed, although rotavirus does not transit through the Golgi apparatus, we have shown that monensin treatment, which is known to inhibit exit from the Golgi, leads to a nonvectorial release of virions. It is well known that GSL are synthesized and sorted in the Golgi. They are incorporated in vesicles that will reach primarily the apical surface with their cargo (29, 45). Upon monensin treatment, the exit from the Golgi of GSL should be perturbed, thus interfering with the production of vesicles destined for the apical side. Since our preliminary studies suggest that rotavirus-containing vesicles interact with the GSL and in this way reach the apical surface, it can be supposed that upon monensin treatment the virus will be transported randomly with no more vectorial release. This working hypothesis will be further elucidated in our next studies.

Vectorial release of virus is of crucial importance for viral pathogenesis. Viruses that enter and are released from epithelial cells at the apical membrane would be restricted to the epithelial surface and produce a localized infection, while nondirectional release from lysed cells or basolateral release may facilitate spreading of the infection to underlying tissue (56). The pathogenesis of rotavirus, with a rather limited tissue tropism, in most cases infecting only the villus epithelium of the small intestine, is in agreement with apical release. However, it has been well established that rotavirus is able to infect cultured cells derived from other tissues, such as kidney or liver (23, 44). Our results suggest that the efficient, highly specific

intestinal tropism of rotavirus is not related to an inability to infect other tissues but results from its vectorial apical release from intestinal cells.

ACKNOWLEDGMENTS

We thank J. Cohen (INRA, Jouy en Josas, France) for kindly providing antirotavirus serum and the RRV strain. We also thank C. Sapin for helpful discussions during the preparation of the manuscript and Tiumo Karjalainen for his help with the English. Most of the confocal experiments were performed with the kind cooperation of the Institut federatif de Recherche INSERM "Cellules Epitheliales, CHU X. Bíchat, Paris, France.

REFERENCES

1. **Altenburg, B. C., D. Y. Graham, and M. K. Estes.** 1980. Ultrastructural study of rotavirus replication in cultured cells. J. Gen. Virol. **46:**75–85.
2. **Anderson, G. W. J., and J. F. Smith.** 1987. Immunoelectron microscopy of Rift Valley fever viral morphogenesis in primary rat hepathocytes. Virology **161:**97–100.
3. **Bacher, A., K. Griebl, S. Mackamul, R. Mitreiter, H. Muckter, and Y. Benshaul.** 1992. Protease inhibitor suppress the formation of tight junctions in gastrointestinal cells. Exp. Cell Res. **200:**97–104.
4. **Baricault, L., M. Garcia, C. Cibert, C. Sapin, G. Geraud, P. Codogno, and G. Trugnan.** 1993. Forskolin blocks the apical expression of dipeptidyl peptidase IV in Caco-2 cells and induces its retention in lamp-1-containing vesicles. Exp. Cell Res. **209:**277–287.
5. **Bishop, R. F., G. P. Davidson, I. H. Holmes, and B. J. Ruck.** 1973. Virus particles in epithelial cells of duodenal mucosa from children with acute non-bacterial gastroenteritis. Lancet **2:**1281–1283.
6. **Bridger, J. C., B. Burke, G. M. Beards, and U. Desselberger.** 1992. The pathogenicity of two porcine rotaviruses differing in their in vitro growth characteristics and genes 4. J. Gen. Virol. **73:**3011–3015.
7. **Carlsson, S. R., J. Roth, F. Piller, and M. Fukuda.** 1988. Isolation and characterization of human lysosomal membrane glycoproteins, h-lamp-1 and h-lamp-2. J. Biol. Chem. **263:**18911–18919.
8. **Chen, S. Y., Y. Matsuoka, and R. W. Compans.** 1991. Assembly and polarized release of punta toro virus and effects of brefeldin A. J. Virol. **65:**1427–1439.
9. **Clark, S. M., J. R. Roth, M. L. Clark, B. B. Barnett, and R. S. Spendlove.** 1981. Trypsin enhancement of rotavirus infectivity: mechanism of enhancement. J. Virol. **39:**816–822.
10. **Clayson, E. T., L. V. J. Brando, and R. W. Compans.** 1989. Release of simian Virus 40 virions from epithelial cells is polarized and occurs without cell lysis. J. Virol. **63:**2278–2288.
11. **Elliott, G., and P. O'Hare.** 1997. Intracellular trafficking and protein delivery by a Herpesvirus structural protein. Cell **88:**223–233.
12. **Estes, M. K.** 1996. Rotaviruses and their replication, p. 1625–1655. *In* B. N. Fields and D. M. Knipe (ed.), Fields' virology, vol. 1. Raven Press, New York, N.Y.
13. **Estes, M. K., and D. Y. Grahan.** 1980. Identification of rotaviruses of different origins by plaque reduction test. Am. J. Vet. Res. **41:**8–14.
14. **Fantini, J., S. Baghdiguian, N. Yahi, and J. C. Chermann.** 1991. Selected human immunodeficiency virus replicates preferentially through the basolateral surface of differentiated human colon epithelial cells. Virology **185:** 904–905.
15. **Fogh, J., J. M. Fogh, and T. Orfeo.** 1977. One hundred and twenty seven cultured human tumor cell lines producing tumor in nude mice. J. Natl. Cancer Inst. **59:**221–226.
16. **Garcia, M., C. Mirre, A. Quaroni, H. Reggio, and A. Le Bivic.** 1993. GPI anchored proteins associate to form microdomains during their intracellular transport in Caco-2 cells. J. Cell Sci. **104:**1281–1290.
17. **Gorvel, J. P., A. Ferrero, L. Chanbraud, A. Rigal, J. Bonicel, and S. Maroux.** 1991. Expression of sucrase-isomaltase and dipeptidylpeptidase IV in human small intestine and colon. Gastroenterology **101:**618–625.
18. **Gottlieb, T. A., A. Gonzalez, L. Rizzolo, M. J. Rindler, M. Adesnik, and D. D. Sabatini.** 1986. Sorting and endocytosis of viral glycoproteins in transfected polarized epithelial cells. J. Cell Biol. **102:**1242–1255.
19. **Holtzman, E.** 1989. Lysosomes. Plenum Press, New York, N.Y.
20. **Jourdan, N., J. Cotte-Laffitte, F. Forestier, A. L. Servin, and A. M. Quero.** 1995. Infection of cultured human intestinal cells by monkey RRV and human Wa rotavirus as a function of intestinal epithelial cell differentiation. Res. Virol. **146:**325–331.
21. **Kabcenell, A. K., and P. H. Atkinson.** 1985. Processing of the rough endoplasmic reticulum membrane glycoproteins of rotavirus SA11. J. Cell Biol. **101:**1270–1280.
22. **Kapikian, A. Z., and R. M. Shanock.** 1996. Rotaviruses, p. 1657–1708. *In* B. N. Fields and D. M. Knipe (ed.), Fields' virology. Raven Press, New York, N.Y.
23. **Kitamoto, N., R. F. Ramig, D. O. Matson, and M. K. Estes.** 1991. Comparative growth of different rotavirus strains in differentiated cells (MA104, HepG2, and Caco-2). Virology **184:**729–737.
24. **Kundu, A., R. T. Avalos, C. M. Sanderson, and D. P. Nayak.** 1996. Transmembrane domain of influenza virus neuraminidase, a type II protein, possesses an apical sorting signal in polarized MDCK cells. J. Virol. **70:**6508–6515.
25. **McQueen, N. L., D. P. Nayak, E. B. Stephens, and R. W. Compans.** 1986. Polarized expression of a chimeric protein in which the transmembrane and cytoplasmic domains of the influenza virus hemagglutinin have been replaced by those of the vesicular stomatitis virus. Proc. Natl. Acad. Sci. USA **83:**9318–9322.
26. **Menard, R., C. C. Dehio, and P. Sansonetti.** 1996. Bacterial entry into epithelial cells, the paradigm of Shigella. Trends Microbiol. **4:**220–226.
27. **Mengaud, J., H. Ohayon, P. Gounon, R. M. Mege, and P. Cossart.** 1996. E-cadherin is the receptor for internalin, a surface protein required for entry of L. monocytogenes into epithelial cells. Cell **84:**923–932.
28. **Mirazimi, A., C.-H. Von Bonsdorf, and L. Svensson.** 1996. Effect of brefeldin A on rotavirus assembly and oligosaccharide processing. Virology **217:**554–563.
29. **Mirre, C., L. Monlauzeur, M. Garcia, M. H. Delgrossi, and A. Le Bivic.** 1996. Detergent-resistant membrane microdomains from Caco-2 cells do not contain caveolin. Am. J. Physiol. **40:**C887–C894.
30. **Musalem, C., and R. T. Espero.** 1985. Release of progeny virus from cell infected with simian rotavirus SA11. J. Gen. Virol. **66:**2715–2724.
31. **Owens, R. J., J. W. Dubay, E. Hunter, and R. W. Compans.** 1991. Human immunodeficiency virus envelope protein determines the site of virus release in polarized epithelial cells. Proc. Natl. Acad. Sci. USA **88:**3987–3991.
32. **Petrie, B. L., D. Y. Graham, H. Hanssen, and M. K. Estes.** 1982. Localisation of rotavirus antigens in infected cells by ultrastructural immunochimistry. J. Gen. Virol. **63:**457–467.
33. **Petrie, B. L., H. B. Greenberg, D. Y. Graham, and M. K. Estes.** 1984. Ultrastructural localization of rotavirus antigens using colloidal gold. Virus Res. **1:**133–152.
34. **Pinto, M., S. Robine-Leon, M. D. Appay, M. Kedinger, N. Triadou, E. Dussaulx, B. Lacroix, P. Simon-Aussman, K. Haffen, J. Fogh, and A. Zweibaum.** 1983. Enterocyte-like differentiation and polarization of the human colon carcinoma cell line Caco-2 in culture. Biol. Cell **47:**323–330.
35. **Pressman, B. C.** 1976. Biological applications of ionophores. Annu. Rev. Biochem. **45:**501–530.
36. **Rodriguez-Boulan, E., and M. Pendergast.** 1980. Polarized distribution of viral envelope proteins in the plasma membrane of infected epithelial cells. Cell **20:**45–54.
37. **Rodriguez-Boulan, E., and D. D. Sabatini.** 1978. Asymmetric budding of viruses in epithelial monolayers: a model system for study of epithelial polarity. Proc. Natl. Acad. Sci. USA **75:**5071–5075.
38. **Rolsma, M. D., H. B. Gelberg, and M. S. Kuhlenschidt.** 1994. Assay for evaluation of rotavirus cell-interactions: identification of an enterocyte ganglioside fraction that mediates group A porcine rotavirus recognition. J. Virol. **68:**258–268.
39. **Rossen, J. W. A., C. P. J. Bekker, W. F. Voorhout, G. J. A. M. Strous, A. van der Ende, and P. J. M. Rottier.** 1994. Entry and release of transmissible gastroenteritis coronavirus are restricted to apical surfaces of polarized epithelial cells. J. Virol. **68:**7966–7973.
40. **Rossen, J. W. A., W. F. Voorhout, M. C. Horzinek, A. van der Ende, G. J. A. M. Strous, and P. J. M. Rottier.** 1995. MHV-A59 enters polarized murine epithelial cells through the apical surface but is released basolaterally. Virology **210:**54–66.
41. **Roth, M. G., R. W. Compans, L. Giusti, A. R. Davis, D. P. Nayak, M. J. Gething, and J. Sambrook.** 1983. Influenza virus hemagglutinin expression is polarized in cells infected with recombinant SV 40 viruses carrying cloned hemagglutinin DNA. Cell **33:**435–443.
42. **Roth, M. G., D. Gunderson, N. Patil, and E. Rodriguez-Boulan.** 1987. The large external domain is sufficient for the correct sorting of secreted or chimeric influenza virus hemagglutinin in polarized monkey kidney cells. J. Cell Biol. **104:**769–782.
43. **Roth, M. G., R. V. Srninivas, and R. W. Compans.** 1983. Basolateral maturation of retroviruses in polarized epithelial cells. J. Virol. **45:**1065–1070.
44. **Schwarz, K. B., T. J. Moore, R. K. Willoughby, Jr., S. B. Wee, S. L. Wonderfecht, and R. H. Yolken.** 1990. Growth of group A rotaviruses in a human liver cell line. Hepathology **12:**638–643.
45. **Simons, K., and A. Wandinger-Ness.** 1990. Polarized sorting in epithelia. Cell **62:**207–210.
46. **Srinivas, R. V., N. Balachandran, F. V. Alonso-Caplen, and R. W. Compans.** 1986. Expression of herpes simplex virus glycoproteins in polarized epithelial cells. J. Virol. **58:**689–693.
47. **Stein, M. A., D. A. Mathers, H. Yan, K. G. Bainbridge, and B. B. Finlay.** 1996. Enteropathogenic *Escherichia coli* markedly decreases the resting membrane potential of Caco-2 and HeLa human epithelial cells. Infect. Immun. **64:**4820–4825.
48. **Suomalainen, M., K. Hultemby, and H. Garoff.** 1996. Targeting of Moloney murine leukemia virus gag precursor to the site of virus budding. J. Cell Biol. **135:**1841–1852.

49. **Superti, F., and G. Donelli.** 1995. Characterization of SA-11 rotavirus receptorial structures on human colon carcinoma cell line HT-29. J. Med. Virol. **47:**421–428.
50. **Superti, F., and G. Donelli.** 1991. Gangliosides as binding sites in SA-11 rotavirus infection of LLC-MK2 cells. J. Gen. Virol. **72:**2467–2474.
51. **Suzuki, H., S. Kitaoka, T. Konno, T. Sato, and N. Ishida.** 1985. Two modes of human rotavirus entry into MA 104 cells. Arch. Virol. **85:**25–34.
52. **Svensson, L., B. B. Finlay, D. Bass, C. H. vonBonsdorff, and H. B. Greenberg.** 1991. Symmetric infection of rotavirus on polarized human intestinal epithelial (Caco-2) cells. J. Virol. **65:**4190–4197.
53. **Tartakof, A., and P. Vassalli.** 1983. Lectin-binding sites as markers of Golgi subcompartement: proximal to distal maturation of oligosaccharides. J. Cell Biol. **97:**1243–1248.
54. **Tartakoff, A. M.** 1986. Temperature and energy dependence of secretory protein transport in the exocrine pancreas. EMBO J. **5:**1477–1482.
55. **Tashiro, M., E. Pritzer, M. A. Kosman, M. Yamakawa, K. Kuroda, H. D. Klenk, R. Rott, and J. T. Seto.** 1988. Characterization of a pantropic variant of Sendai virus derived from a host range mutant. Virology **165:**577–583.
56. **Tashiro, M., M. Yamakawa, K. Tobita, J. T. Seto, H. D. Klenk, and R. Rott.** 1990. Altered budding site of a pantropic mutant of Sendai virus, F1-R, in polarized epithelial cells. J. Virol. **64:**4672–4677.
57. **Theil, K. W., E. H. Bohl, R. F. Cross, E. M. Kohler, and A. G. Agnes.** 1978. Pathogenesis of porcine rotaviral infection in experimentally inoculated gnotobiotic pigs. Am. J. Vet. Res. **39:**213–220.
58. **Tian, P., J. M. Ball, C. Q. Y. Zeng, and M. K. Estes.** 1996. The rotavirus nonstructural glycoprotein NSP4 possesses membrane destabilization activity. J. Virol. **70:**6973–6981.
59. **Trugnan, G., M. Rousset, I. Chantret, A. Barbat, and A. Zweibaum.** 1987. The posttranslational processing of sucrase-isomaltase in HT-29 cells is a function of their state of enterocyte differentiation. J. Cell Biol. **104:**1199–1205.
60. **Tucker, S. P., and R. W. Compans.** 1993. Virus infection of polarized epithelial cells. Adv. Virus Res. **42:**187–247.
61. **Tucker, S. P., C. L. Thornton, E. Wimmer, and R. W. Compans.** 1993. Vectorial release of poliovirus from polarized human intestinal epithelial cells. J. Virol. **67:**4274–4282.
62. **Willoughby, R. E., R. H. Yolken, and R. L. Schnaar.** 1990. Rotavirus specifically bind to the neutral glycosphingolipid asialo-GM1. J. Virol. **64:**4830–4835.